

Communications

Electric Field of a Six-Needle Array Electrode Used in Drug and DNA Delivery *In Vivo*: Analytical Versus Numerical Solution

Sukhendu B. Dev, Deepak Dhar, and Wanda Krassowska*

Abstract—We present an analytical solution for the electrical potential and field established by a six-needle array electroporation electrode, which is used *in vivo* for cancer treatment and DNA delivery. The analytical solution closely matches the numerical solution obtained with the finite element method: the mean error is less than 0.6%.

Index Terms—Electroporation, electric field, finite element, multipole expansion.

I. INTRODUCTION

Electroporation is a technique that uses pulsed electric fields to deliver drugs and genetic material to cells. In the last ten years, electroporation has been applied clinically to treat localized cancers [1]–[12] and efforts are under way to extend it to gene therapy [13]–[17]. However, success of the electroporation-based treatment depends on the electrode configuration and the pulsing protocol. Of the different electrode configurations tried, the most successful has been the six-needle array [5], [18], shown in Fig. 1. During a typical electroporation therapy, an intratumoral or intravenous injection of an anticancer drug is followed by an application of a short (100 μ s) pulse between two adjacent needles (e.g., needles 2–3) and their opposite pair (e.g., needles 5–6). Next, an identical pulse is applied through another two pairs of needles, rotated by 60° from the first set (e.g., 3–4 and 6–1). Four more pulses rotated by 60° follow, until the whole tumor has been exposed. While different electrodes are active during different pulses of this sequence, it is mainly the maximum electric field that determines the outcome of the treatment [19]–[21]. Hence, the strength of the electric field to which the treated tissue is exposed is one of the most important parameters for the proper design and optimization of pulsing protocols.

Most commonly, electric fields for different electrode configurations are estimated numerically, using a finite element or a finite difference method [5], [20]–[25], although an analytical solution for the two-needle configuration is known [26]. In our study, we use the multipole expansion [27] to derive an analytical solution for the potential and field of a six-needle array electrode (Fig. 1). The leading order term and the first correction terms are explicitly determined. In principle, it is straightforward to determine higher order corrections; however, these corrections are found to be negligible. The analytical solution is compared with the numerical solution obtained with the commercial finite element program PDEase [28]. The analytical solution is of practical interest because it provides a convenient way to estimate the electric

Manuscript received June 6, 2002; revised April 3, 2003. This work was supported in part by the National Science Foundation (NSF) under Grant BES-9974185 and Grant BES-0108408. *Asterisk indicates corresponding author.*

S. B. Dev is with Gene Delivery & Expression Sciences, San Diego, CA 92122 USA.

D. Dhar is with the Department of Theoretical Physics, Tata Institute of Fundamental Research, Mumbai 400005, India.

*W. Krassowska is with the Department of Biomedical Engineering, Duke University, Durham, NC 27708-0281 USA (e-mail: wanda.krassowska@duke.edu).

Digital Object Identifier 10.1109/TBME.2003.818467

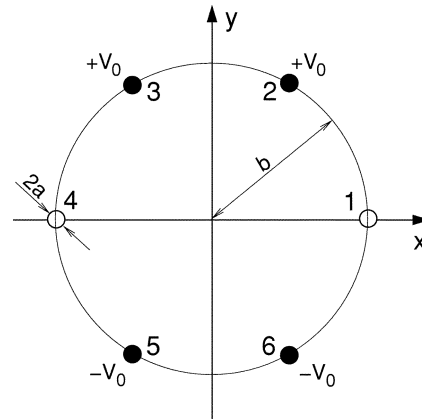


Fig. 1. Electroporation electrode consisting of an array of six needles of radius a placed equidistantly on a circle of radius b . This figure shows the configuration for the first pulse: black circles represent cross-sections of active electrodes, kept at potentials V_0 or $-V_0$, and white circles represent cross sections of electrodes kept at zero potential.

field of the six-needle array electrode, which is used in pre-clinical experiments and clinical treatments of localized cancers and in gene delivery [5], [18], [21], [23], [29], [30].

II. METHODS

A. Analytical Solution

If the needles are long, of uniform thickness, and fully inserted into the tumor, the potential can be considered two-dimensional away from the tips of the needles. Thus, we can examine the distribution of potential on a plane. Needles are represented as circles of radius a . We shall obtain the solution for the case when needles 2 and 3 are kept at potential $+V_0$, needles 5 and 6 at $-V_0$, and needles 1 and 4 at zero (Fig. 1). Solutions for pulsing configurations in which other electrodes are active are related to this solution by rotational symmetry. Assuming that the tissue can be represented as a medium of constant conductivity, the potential $\Phi(x, y)$ in the entire region outside the needles is the solution of Laplace's equation

$$\nabla^2 \Phi(x, y) = 0 \quad (1)$$

where Φ vanishes at infinity and takes prescribed values at the needles' boundaries. Introducing the complex variable $z = x + iy$, we look for a complex analytic function, $\Phi(z)$, such that its real part, $\text{Re}[\Phi(z)]$, takes the prescribed values on the needles and automatically satisfies Laplace's equation throughout the region. Hence, $\Phi(x, y) = \text{Re}[\Phi(z)]$ is the desired solution.

By superposition, the total potential is the sum of potentials generated by each needle

$$\Phi(z) = \sum_{n=1}^6 \Phi_n(z) \quad (2)$$

where

$$\Phi_n(z) = C_n \log \frac{a}{z - z_n} + \sum_{k=1}^{\infty} A_{nk} \left(\frac{a}{z - z_n} \right)^k \quad (3)$$

is the potential generated by the n th needle. In this expansion, the first term represents a potential established by a monopole source located

at the center of the n th needle, i.e., at $z_n = be^{i(n-1)\pi/3}$, where b is the radius of the needle array (Fig. 1). The terms with $k = 1, 2, 3, \dots$ correspond to the dipole, quadrupole, octapole, etc. moments of the uneven charge distribution on the n th needle. For $b \gg a$, the effect of these terms decreases very rapidly with k , allowing us to obtain a good approximation with only two terms.

B. Leading-Order Potential and Electric Field

The leading order approximation to the solution is obtained by retaining only the monopole term in (3) and neglecting the sum over k . By symmetry, coefficients C_n are

$$C_1 = C_4 = 0, \quad C_2 = C_3 = -C_5 = -C_6 = C \quad (4)$$

where C is a constant to be determined from the boundary conditions. By combining the first term of (3) and (4), the leading-order potential generated by all needles becomes

$$\Phi^0(z) = C \log \frac{(z - z_5)(z - z_6)}{(z - z_2)(z - z_3)}. \quad (5)$$

To determine constant C , consider the boundary of needle 2. The position of any point on this boundary can be specified as $z = z_2 + ae^{i\varphi}$. Using notation $z_{nk} = z_n - z_k$ and taking into consideration that needle radius, a , is much smaller than the distance between any two electrodes, $z - z_5 = z_{25} + ae^{i\varphi} \approx z_{25}$, $z - z_6 \approx z_{26}$, and $z - z_3 \approx z_{23}$, while $z - z_2 = ae^{i\varphi}$. Values of z_{25} , z_{26} , and z_{23} are determined from the geometry of the needle array (Fig. 1). Introducing z_{25} , z_{26} , and z_{23} values to (5) and taking into account that the potential on needle 2 is equal to V_0 , constant C is found to be

$$C = \frac{V_0}{\log(2\sqrt{3}\frac{b}{a})}. \quad (6)$$

Differentiating (5) with respect to z , we obtain the leading-order approximation for the electric field. The field strength is

$$E^0(z) = C \left(\frac{1}{z - z_5} + \frac{1}{z - z_6} - \frac{1}{z - z_2} - \frac{1}{z - z_3} \right). \quad (7)$$

C. First-Order Correction

First-order correction to the solution includes the dipole moment terms (i.e., terms of the sum in (3) corresponding to $k = 1$) and neglects the higher order terms of expansion (3). Thus, the solution that includes the leading-order and the first-order terms is

$$\Phi^1(z) = C \log \frac{(z - z_5)(z - z_6)}{(z - z_2)(z - z_3)} + a \sum_{n=1}^6 \frac{A_{n1}}{z - z_n}. \quad (8)$$

The coefficients A_{n1} are determined from the constant potential prescribed on the surface of the needles. Here, we show in detail computations of A_{11} . The potential at a point on the surface of needle 1, i.e., at $z = z_1 + ae^{i\varphi}$, is

$$\Phi^1(z_1 + ae^{i\varphi}) = C \log \frac{(z_1 - z_5 + ae^{i\varphi})(z_1 - z_6 + ae^{i\varphi})}{(z_1 - z_2 + ae^{i\varphi})(z_1 - z_3 + ae^{i\varphi})} + \sum_{n=1}^6 A_{n1} \frac{a}{z_1 - z_n + ae^{i\varphi}}. \quad (9)$$

Expanding in Taylor series and keeping only $O(a/b)$ terms, we approximate

$$\log(z_1 - z_n + ae^{i\varphi}) \approx \log(z_{1n}) + \frac{ae^{i\varphi}}{z_{1n}}. \quad (10)$$

Likewise, in the sum, we keep only $O(a/b)$ terms, which eliminates terms with $n \neq 1$. Hence, (9) becomes

$$\Phi^1(z_1 + ae^{i\varphi}) = C \log \frac{z_{15}z_{16}}{z_{12}z_{13}} + Cae^{i\varphi} \left(\frac{1}{z_{15}} + \frac{1}{z_{16}} - \frac{1}{z_{12}} - \frac{1}{z_{13}} \right) + A_{11}e^{-i\varphi}. \quad (11)$$

A_{11} is determined from the boundary condition $\text{Re}[\Phi^1(z_1 + ae^{i\varphi})] = 0$, for all φ . Since $(z_{15}z_{16})/(z_{12}z_{13}) = 1$ and $\text{Re}[A_{11}ae^{-i\varphi}] = \text{Re}[A_{11}^*ae^{i\varphi}]$, the formula for the complex conjugate of A_{11} , A_{11}^* , is

$$A_{11}^* = -C \left(\frac{1}{z_{15}} + \frac{1}{z_{16}} - \frac{1}{z_{12}} - \frac{1}{z_{13}} \right). \quad (12)$$

After evaluating z_{15} , z_{16} , z_{12} and z_{13} from Fig. 1, $A_{11}^* = iC(4/\sqrt{3})(a/b)$ and therefore, $A_{11} = -iC(4/\sqrt{3})(a/b)$. Similar calculations have been performed to give all coefficients as

$$\begin{aligned} A_{11} = A_{41} &= -iC \frac{a}{b} \frac{4}{\sqrt{3}} \\ A_{21} = A_{51} &= C \frac{a}{b} \left(\frac{3}{4} - i \frac{7}{4\sqrt{3}} \right) \\ A_{31} = A_{61} &= C \frac{a}{b} \left(-\frac{3}{4} - i \frac{7}{4\sqrt{3}} \right). \end{aligned} \quad (13)$$

With all coefficients determined, the first-order accurate expression for the electric field can be computed by differentiating (8) with respect to z . The field strength is

$$E^1(z) = C \left(\frac{1}{z - z_5} + \frac{1}{z - z_6} - \frac{1}{z - z_2} - \frac{1}{z - z_3} \right) + a \sum_{n=1}^6 \frac{A_{n1}}{(z - z_n)^2}. \quad (14)$$

Distributions of potential and electric field magnitude were computed from (5), (7), (8), and (14) as follows. The geometry of the six-needle array was as shown in Fig. 1, with needle radius a equal to 0.215 mm and the radius of the array b equal to 5 mm. The voltage on the four active needles, V_0 , was 0.5 V, so that the potential difference between the two opposite-polarity needle pairs was 1 V. The voltage on the remaining two needles was 0 V. Because the model is linear, the solution for the kilovolt-level pulses commonly used in electrochemotherapy can be obtained by scaling.

The potential and field strength were analyzed throughout a square region of dimensions $2b \times 2b$, i.e., twice the diameter of the needle array. This region was covered by a grid of 186×186 nodes, $a/4$ (0.053 57 mm) apart. A program written in Matlab [31] computed and displayed the potential and the field strength at each node of this grid.

D. Numerical Solution

Numerical estimates of the potential and electric field were obtained using the finite-element method. Laplace's (1), subject to the prescribed boundary conditions, was solved using the commercial software package PDEase ([28]; available: <http://www.macsyma.com>). The dimensions of the needles and the array were the same as in the analytical solution described above. The surfaces of the needles were represented as circles and assigned Dirichlet boundary conditions with a constant potential of 0.5 or -0.5 V for the four active needles and 0 V for the remaining two needles. Since PDEase can compute solutions only for regions of finite extent, the needle array was positioned in the center of a circle of radius R_{outer} equal to $2b$. No-flux boundary condition was applied on the boundary of this circle. The effect of this no-flux boundary was estimated as follows: when R_{outer} was increased by a factor of two, the potential along the path between needles 2 and 6 changed by 0.0276 (mean error, computed as an L_2 norm of the difference divided by the L_2 norm of the potential).

PDEase uses automatic adaptive grid refinement to achieve the desired accuracy. For this problem, an irregular grid consisting of 2127 nodes and 1014 elements was generated. The mean error of the numerical solution, estimated by PDEase across all elements, was 3.7×10^{-4} .

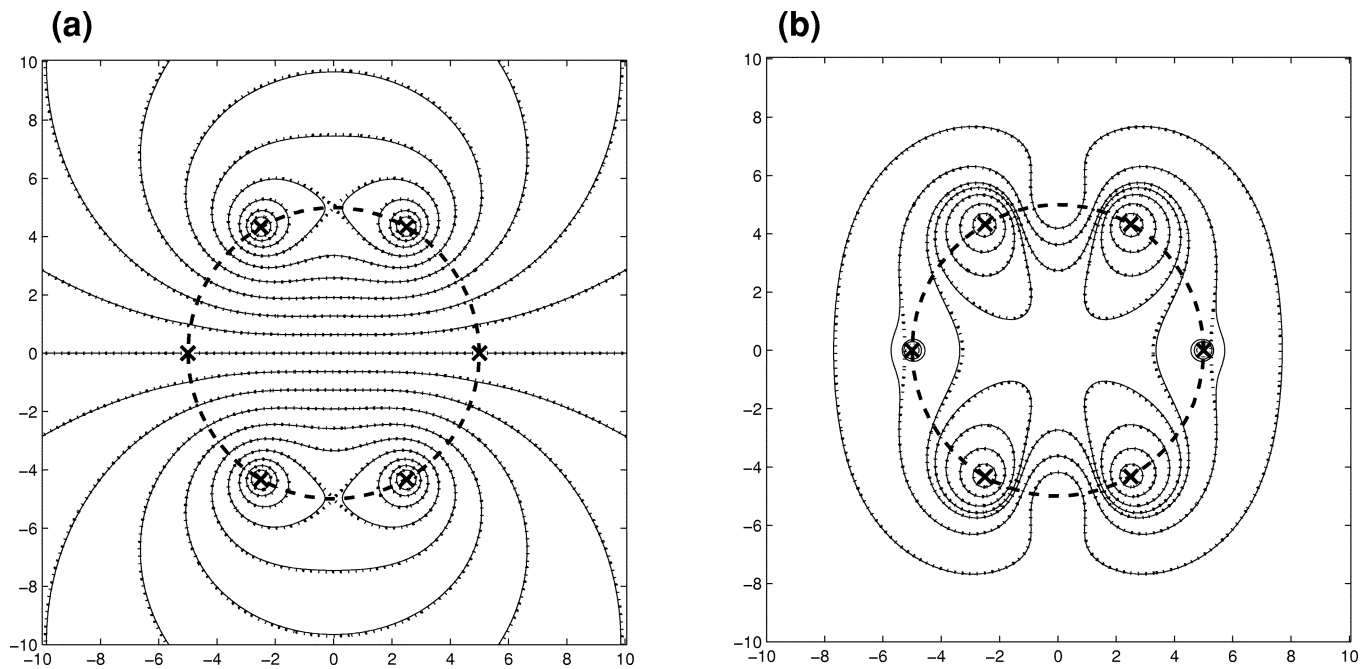


Fig. 2. Contour plots of a leading-order potential (real part of (5), dotted lines) and a first-order accurate potential (real part of (8), solid lines). Contours are drawn at $-0.5, -0.45, -0.4, \dots, 0.4, 0.45, 0.5$ V. (b) Contour plots of a leading-order field strength (real part of (7), dotted lines) and a first-order accurate field strength (real part of (14), solid lines). Contours are drawn at $0.03, 0.05, 0.07, 0.08, 0.1, 0.15,$ and 0.3 V/mm. In both panels, the voltage on positive needles is 0.5 V and on negative needles is -0.5 V, dashed circle is the circumference of the needle array, and positions of the needles are marked with an "x".

III. RESULTS

A. Analytical Solution

Fig. 2(a) compares the leading-order and the first-order accurate solutions for potential, $\tilde{\Phi}^0(x, y)$ and $\tilde{\Phi}^1(x, y)$ [real parts of (5) and (8)]. In both cases, the magnitude of the potential is the highest on the surface of the active needles (0.5 and -0.5 V) and decreases with the distance from the needle. The equipotential lines in the middle of the electrode array are approximately parallel and equally spaced, indicating that the electric field in this region is approximately constant. There are only minor differences between these two plots, demonstrating that even the leading-order approximation alone is fairly accurate. The mean error between $\tilde{\Phi}^0(x, y)$ and $\tilde{\Phi}^1(x, y)$, calculated over all nodes inside the needle array, is 1.47×10^{-5} ; the maximum difference is 0.002 V.

To see the role of the first-order correction, one must examine $\tilde{\Phi}^0(x, y)$ and $\tilde{\Phi}^1(x, y)$ along the circumference of the needles, as shown in Fig. 3 for needle 2. Because $\tilde{\Phi}^0(x, y)$ corresponds to the monopole sources, the potential along the circumference of each needle exhibits sinusoidal variations. Adding the first-order correction essentially eliminates the azimuthal variations of potential: $\tilde{\Phi}^1(x, y)$ is nearly constant. This figure also shows that the value of $\tilde{\Phi}^1(x, y)$ is very close to the assigned boundary conditions of 0.5 V.

Fig. 2(b) compares the leading-order and the first-order accurate solutions for the strength of the electric field, \tilde{E}^0 and \tilde{E}^1 [real parts of (7) and (14)]. In both cases, the field is the highest on the surface of the active needles, reaching a magnitude of 0.6 V/mm. Note a small perturbation in the field caused by the presence of inactive needles, 1 and 4. The middle of the electrode array is exposed to a field of the magnitude $2\sqrt{3}V_0/(b \log(2\sqrt{3}b/a)) = 0.0789$ V/mm. The mean error between \tilde{E}^0 and \tilde{E}^1 over all nodes inside the array is 1.84×10^{-4} ; the maximum difference is 0.005 V/mm.

B. Comparison of Analytical and Numerical Solutions

The contour plots of the potential and field strength, obtained from the finite element model, are very similar to the plots shown in Fig. 2

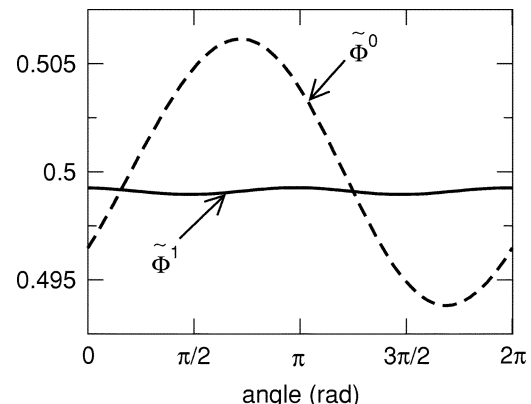


Fig. 3. Leading-order and first-order accurate potential plotted as a function of position along the circumference of needle 2.

and therefore, are not shown. Fig. 4(a), (c), (e) compares the numerical solution for potential with the first-order accurate analytical solution $\tilde{\Phi}^1(x, y)$, by plotting them along three different paths bisecting the array. In a similar manner, Fig. 4(b), (d), (f) compares the electric fields. Inside the electrode array, the mean error between numerical and analytical solutions is less than 0.6% : 5.6×10^{-3} between potentials and 5.5×10^{-3} between field strengths; the maximum differences are 0.032 V and 0.028 V/mm, respectively. If only the leading-order analytical solution is used, the errors are essentially the same.

Outside the electrode array, the discrepancy between analytical and numerical solution increases. This discrepancy is due to the fact that the finite element model represents only a finite region, with the no-flux boundary condition on the outer boundary, R_{outer} . Changing R_{outer} from $2b$ (twice the radius of the array) to $3b$ reduces the error between analytical and numerical solution by a factor of two (Fig. 4, solid vs. dotted lines). However, R_{outer} cannot be made much larger without a decrease in overall accuracy caused by the large difference in size between the smallest and the largest object (needles versus the entire region). The analytical solution, which assumes an infinite region, avoids this problem altogether.

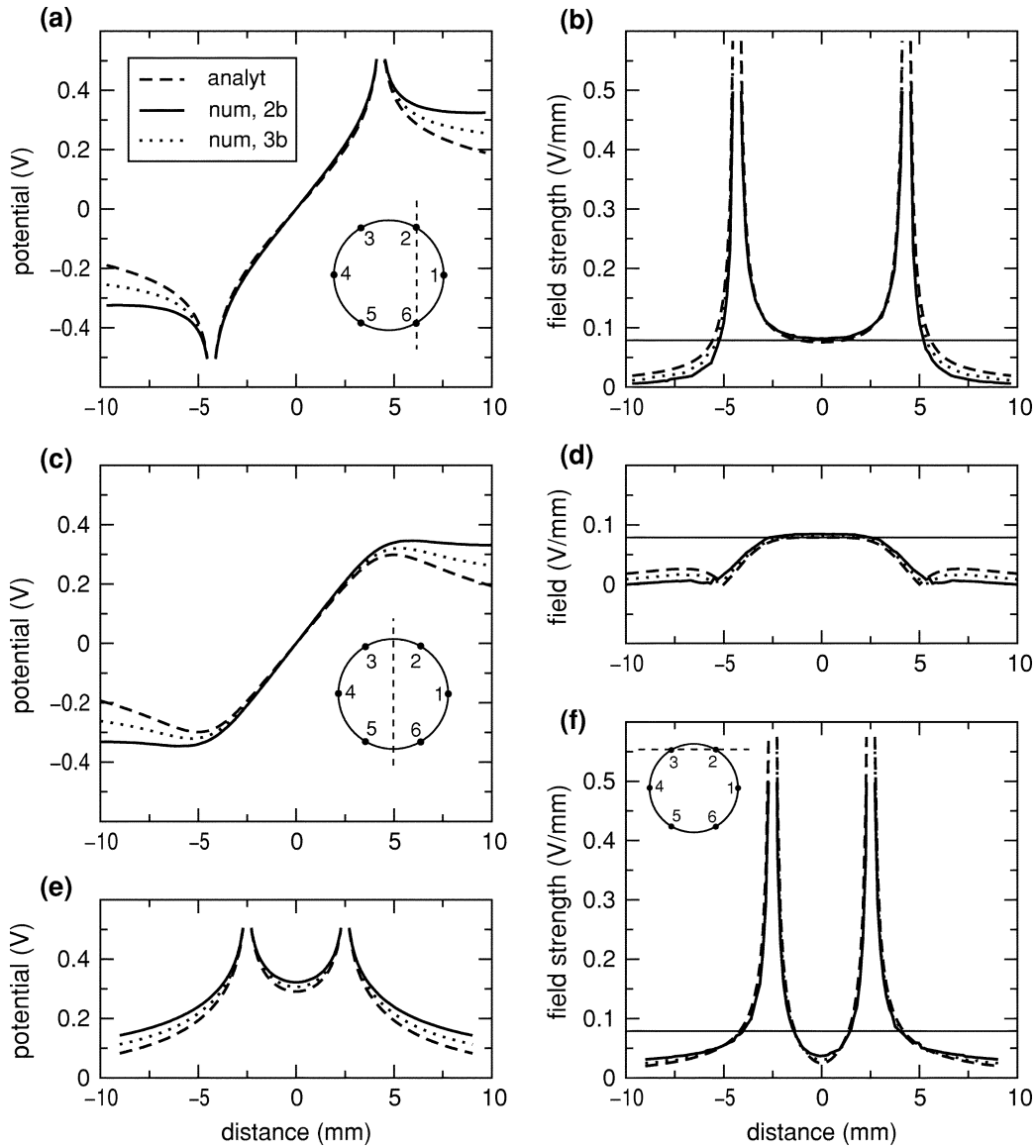


Fig. 4. Analytic and numerical solutions for potential and field strength plotted as a function of position along three different paths (shown in insets). (a-b) Path through needles 6 and 2, (c-d) path through the center of the array, and (e-f) path through needles 3 and 2. For the numerical solution, two different region sizes were used: $R_{\text{outer}} = 2b$ (solid line) and $R_{\text{outer}} = 3b$ (dotted line).

IV. DISCUSSION

This study presents an analytical solution for the potential and field generated by a six-needle electroperoration electrode. The multipole expansion series converges rapidly, and dropping second and higher order terms causes negligible error. In fact, even a leading-order approximation gives a very accurate approximation of the electric field distribution. This solution closely matches the numerical approximation computed using the finite element method: the mean error between the two fields is less than 0.6%. The series solution has an advantage for electric field computations because the derivative is computed analytically, thus avoiding numerical differentiation, which is notoriously error-prone. In consequence, plots of electric fields computed analytically are smooth, while the numerical estimate, in which discretization error is amplified by numerical differentiation, exhibits some ripples [Fig. 4(d), (f)].

The most important limitation of the analytical solution presented here is the restriction of the problem to two dimensions. It gives a good approximation of the electric field along the shafts of the needles, but not close to the tips. When it is important to evaluate the electrical conditions near the needle tips, a finite element program that allows

computation of electric fields in three dimensions, such as ANSYS from Swanson Analysis Systems, Inc. or ECRIT from Field Precision, should be used. In addition, the model assumes uniform and isotropic conductivity. Most tissues exhibit some degree of inhomogeneity and anisotropy [32], and the electric pulse itself can affect the conductivity [33], [34]. While the first two factors can be accounted for in a standard finite element model, the last one cannot: the dynamic changes in conductivity caused by electroperoration would require writing a dedicated program [35].

The results presented in this paper have confirmed previous reports [5], [21]–[23], [25] that nonuniformity of the electric field produced by needle arrays used in clinical practice is very significant and should not be ignored. For the needle geometry studied in this paper, the field strength at the surface of the needle is about six times larger than at the center of the array. A naive estimate of the magnitude of the electric field, obtained by dividing voltage difference (1 V) by the distance between the two pairs of active needles (8.66 mm center-to-center or 8.23 mm surface-to-surface), yields 0.115 V/mm (0.122 V/mm, respectively). For the center of the array, these values represent a nearly 45% (54%, respectively) overestimation, and they underestimate the field

near the needles by a factor of about six. Many experimental studies indicate that the electric field distribution around the needles is very important for the intracellular delivery of drugs and genes. Therefore, detailed quantitative understanding of the electric field established by the electrodes is needed for both the design of the electroporation treatments and for the interpretation of the results.

The formulas developed here provide a convenient way of estimating the distribution of the electric field established by a clinically used electroporation electrode. While the formulas are for a specific number and location of electrodes, the method is general and it can be easily applied to other electrode configurations, as well as to a different number and positions of the electrodes. Thus, one can estimate the fields of the electroporation electrodes without necessarily resorting to a numerical solution.

ACKNOWLEDGMENT

This paper is dedicated to the memory of Swapna Dev. Part of this paper was done while S. B. Dev was with Genetronics, Inc., San Diego, CA, and during W. Krassowska's sabbatical at Genetronics, Inc.

REFERENCES

- [1] M. Okino and H. Mohri, "Effects of a high-voltage electrical impulse and an anticancer drug on *in vivo* growing tumors," *Jap. J. Cancer Res.*, vol. 78, pp. 1319–1321, 1987.
- [2] L. M. Mir, M. Belehradek, C. Domenge, S. Orlowski, B. Poddevin, J. Belehradek, Jr., G. S. G. B. Luboinski, and C. Paoletti, "Electrochemotherapy, a novel antitumor treatment: First clinical trial," *C. R. Acad. Sci. III*, vol. 313, pp. 613–618, 1991.
- [3] J. Belehradek, Jr., S. Orlowski, B. Poddevin, C. Paoletti, and L. M. Mir, "Electrochemotherapy of spontaneous mammary tumors in mice," *Eur. J. Cancer*, vol. 27, pp. 73–76, 1991.
- [4] S. B. Dev and G. A. Hofmann, "Electrochemotherapy—A novel method of cancer treatment," *Cancer Treat. Rev.*, vol. 20, pp. 105–115, 1994.
- [5] G. A. Hofmann, S. B. Dev, and G. S. Nanda, "Electrochemotherapy: Transition from laboratory to the clinic," *IEEE Eng. Med. Biol. Mag.*, vol. 15, pp. 124–132, 1996.
- [6] S. B. Dev, G. S. Nanda, Z. An, X. Wang, R. M. Hoffmann, and G. A. Hofmann, "Effective electroporation therapy of human pancreatic tumors implanted in nude mice," *Drug Deliv.*, vol. 4, pp. 293–299, 1997.
- [7] L. M. Mir, L. F. Glass, G. Serša, J. Teissié, C. Domenge, D. Miklavčič, M. J. Jaroszewski, S. Orlowski, D. S. Reintgen, Z. Rudolf, M. Belehradek, R. Gilbert, M.-P. Rols, J. Belehradek, Jr., J. M. Bachaud, R. DeConti, B. Štambuc, M. Čemažar, P. Coninx, and R. Heller, "Effective treatment of cutaneous and subcutaneous malignant tumors by electrochemotherapy," *Br. J. Cancer*, vol. 77, pp. 2336–2342, 1998.
- [8] G. S. Nanda, F. X. Sun, G. A. Hofmann, R. M. Hoffmann, and S. B. Dev, "Electroporation therapy of human larynx tumors HEP-2 implanted in nude mice," *Anticancer Res.*, vol. 18, pp. 999–1004, 1998.
- [9] —, "Electroporation enhances therapeutic efficacy of anticancer drugs: Treatment of human pancreatic tumor in animal model," *Anticancer Res.*, vol. 18, pp. 1361–1366, 1998.
- [10] G. Serša, B. Stabuč, M. Čemažar, D. Miklavčič, and Z. Rudolf, "Electrochemotherapy with cisplatin: The systemic antitumor effectiveness of cisplatin can be potentiated locally by the application of electric pulses in the treatment of malignant melanoma skin metastases," *Melanoma Res.*, vol. 10, pp. 381–385, 2000.
- [11] K. Yoshizato, T. Nishi, T. Goto, S. B. Dev, H. Takeshima, T. Kino, K. Tada, T. Kimura, S. Shiraiishi, M. Kochi, J.-I. Kuratsu, G. A. Hofmann, and Y. Ushio, "Gene delivery with optimized electroporation parameters shows potential for treatment of gliomas," *Int. J. Oncol.*, vol. 16, pp. 899–905, 2000.
- [12] T. Goto, T. Nishi, T. Tamura, S. B. Dev, H. Takeshima, M. Kochi, J.-I. Kuratsu, T. Sakata, G. A. Hofmann, and Y. Ushio, "Highly efficient electrogene therapy of solid tumor by using an expression plasmid for the herpes simplex virus thymidine kinase gene," *Proc. Nat. Acad. Sci.*, vol. 97, pp. 354–359, 2000.
- [13] A. V. Titomirov, S. Sukharev, and E. Kistanova, "In vivo electroporation and stable transformation of skin cells of newborn mice by plasmid DNA," *Biochim. Biophys. Acta*, vol. 1088, pp. 131–134, 1991.
- [14] T. Nishi, K. Yoshizato, H. Takeshima, K. Sato, K. Hamada, I. Kitamura, T. Yoshimura, H. Saya, J. Kuratsu, and Y. Ushio, "High-efficiency *in vivo* gene transfer using intraarterial plasmid DNA injection following *in vivo* electroporation," *Cancer Res.*, vol. 56, pp. 1050–1055, 1996.
- [15] H. Aihara and J. Miyazaki, "Gene transfer into muscle by electroporation *in vivo*," *Nat. Biotechnol.*, vol. 16, pp. 867–870, 1998.
- [16] L. M. Mir, M. F. Bureau, R. Rangara, B. Schwartz, and D. Scherman, "Long-term, high level *in vivo* gene expression after electric pulse-mediated gene transfer into skeletal muscle," *C. R. Acad. Sci. III*, vol. 11, pp. 893–899, 1998.
- [17] L. M. Mir, M. F. Bureau, J. Gehl, R. Rangara, D. Rouy, J. M. Caillaud, P. Delaere, D. Branellec, B. Schwartz, and D. Scherman, "High-efficiency gene transfer into skeletal muscle mediated by electric pulses," *Proc. Nat. Acad. Sci.*, vol. 96, pp. 4262–4267, 1999.
- [18] R. A. Gilbert, M. J. Jaroszeski, and R. Heller, "Novel electrode designs for electrochemotherapy," *Biochim. Biophys. Acta*, vol. 1334, pp. 9–14, 1997.
- [19] G. Serša, M. Čemažar, D. Šemrov, and D. Miklavčič, "Changing electrode orientation improves the efficacy of electrochemotherapy of solid tumor in mice," *Bioelectrochem. Bioenerg.*, vol. 39, pp. 61–66, 1996.
- [20] D. Šemrov and D. Miklavčič, "Calculation of electrical parameters in electrochemotherapy of solid tumor in mice," *Comput. Biol. Med.*, vol. 28, pp. 439–448, 1998.
- [21] G. A. Hofmann, S. B. Dev, S. Dimmer, and G. S. Nanda, "Electroporation therapy: A new approach for the treatment of head and neck cancer," *IEEE Trans. Biomed. Eng.*, vol. 46, pp. 752–759, June 1999.
- [22] D. Miklavčič, K. Beravs, D. Šemrov, M. Čemažar, F. Demšar, and G. Serša, "The importance of electric field distribution for effective *in vivo* electroporation of tissues," *Biophys. J.*, vol. 74, pp. 2152–2158, 1998.
- [23] G. A. Hofmann, S. B. Dev, G. S. Nanda, and D. P. Rabussay, "Electroporation therapy of solid tumors," *Crit. Rev. Ther. Drug Carrier Syst.*, vol. 16, pp. 523–569, 1999.
- [24] K. Brandinsky and I. Daskalov, "Electrical field and current distributions in electrochemotherapy," *Bioelectrochem. Bioenerg.*, vol. 48, pp. 201–208, 1999.
- [25] D. Miklavčič, D. Šemrov, H. Mekid, and L. M. Mir, "A validated model of *in vivo* electric field distribution in tissues for electrochemotherapy and for DNA electrotransfer for gene therapy," *Biochim. Biophys. Acta*, vol. 1523, pp. 73–83, 2000.
- [26] S. Ramo, J. R. Whinnery, and T. Van Duzer, *Fields and Waves in Communication Electronics*. New York: Wiley, 1965.
- [27] P. Henrici, *Applied and Computational Complex Analysis*. New York: Wiley, 1986.
- [28] *PDEase2D, Finite Element Analysis for Partial Differential Equations Reference Manual*, 2 ed. Arlington, MA: Macsyma, 1999.
- [29] R. Heller, M. J. Jaroszewski, L. F. Glass, J. L. Messina, D. P. Rapaport, R. C. DeConti, N. A. Fenske, R. A. Gilbert, L. M. Mir, and D. S. Reintgen, "Phase I/II trial for the treatment of cutaneous and subcutaneous tumors using electrochemotherapy," *Cancer*, vol. 77, pp. 964–971, 1996.
- [30] W. R. Panje, M. P. Hier, G. R. Garman, E. Harrell, A. Goldman, and I. Bloch, "Electroporation therapy for head and neck cancer," *Ann. Oto. Rhino. Laryn.*, vol. 107, pp. 779–785, 1998.
- [31] D. Hanselman and B. Littlefield, *Mastering Matlab. A Comprehensive Tutorial and Reference*. Upper Saddle River, NJ: Prentice-Hall, 1996.
- [32] S. Rush, J. A. Abildskov, and R. McFee, "Resistivity of body tissues at low frequencies," *Circ. Res.*, vol. 12, pp. 40–50, 1963.
- [33] P. M. Ghosh, C. R. Keese, and I. Giaver, "Monitoring electropermeabilization in the plasma membrane of adherent mammalian cells," *Biophys. J.*, vol. 64, pp. 1602–1609, 1993.
- [34] R. Vanbever, U. F. Pliquet, V. Pr at, and J. C. Weaver, "Comparison of the effects of short, high-voltage and long, medium voltage pulses on skin electrical and transport properties," *J. Control. Release*, vol. 69, pp. 35–47, 1999.
- [35] R. V. Davalos, B. Rubinsky, and D. M. Otten, "A feasibility study for electrical impedance tomography as a means to monitor tissue electroporation for molecular medicine," *IEEE Trans. Biomed. Eng.*, pp. 400–403, Apr. 2002.